Analyst

PAPER

View Article Online
View Journal

Cite this: DOI: 10.1039/d3an01488f

Smart sensing flexible sutures for glucose monitoring in house sparrows†

Mossab K. Alsaedi, ‡[a,b] Rachel E. Riccio,‡[b,c] Atul Sharma,‡[b,d] Junfei Xia,[b,d] Rachel E. Owyeung,[b,d] L. Michael Romero[c] and Sameer Sonkusale *[a,b,d,e]

There is a need for flexible chemical sensors for the ecological and physiological research of avian species such as house sparrows (*Passer domesticus*). Current methods in this field are invasive and require multiple physical interactions with the birds. Emerging research in flexible bioelectronics can enable realization of implantable devices that are mechanically compliant with the underlying tissues for continuous real-time sensing *in situ*. However, challenges still remain in forming an intimate flexible interface. One of the promising flexible bioelectronic platforms for tissue-embedded sensing is based on functionalizing surgical sutures or threads. Threads have three-dimensional flexibility, high surface-area-to-volume ratio, inherent wicking properties, and are easily functionalizable using reel-to-reel dip coating. Threads are ideal as they are lightweight, therefore, would not interfere with flight motion and would only require minimal interaction with the bird. However, the challenge remains in achieving a highly conductive yet flexible electrode for electrochemical sensing using materials such as gold. In this study, we address this issue through novel gold deposition directly on thread substrate followed by enzyme immobilization to realize flexible electrochemical glucose biosensors on medical-grade sutures. These sensors were calibrated and tested in a range that is wide enough to include the expected range of glucose concentration in house sparrows (0–8.55 mM). Glucose monitoring in house sparrows will provide insights into energy metabolism and regulation during stress responses. In addition, the stability, repeatability, and selectivity of the sensor were tested with final validation in a real bird. Our innovative gold-coated, thread-based flexible electrochemical glucose sensor can also be used in other small and large animals. This can also be extended to monitoring other metabolites in future.

Received 30th August 2023,
Accepted 3rd October 2023

DOI: 10.1039/d3an01488f

rsc.li/analyst

Introduction

Flexible bioelectronics have become popular in precision health and medicine as they offer seamless electronic-tissue physical contact and comparable mechanical properties (elastic moduli).[1] Threads have previously been utilized in biomedical applications to realize thread-based sensors, transistors, and even drug-delivery platforms.[1–6] Their three-dimensional flexibility ensures seamless integration with underlying tissues and organs and intimate contact with tissue/organ surfaces.[1] Threads are also favorable because of their cleanroom-free and low-cost fabrication processes, mechanical stability and durability, large surface area, and inherent wicking properties.[1,7–11] The ability to select different types of fibers that make up threads also provides flexibility in terms of the application and the desired properties of the thread-based device.[7] Choosing biocompatible fibers, such as silk and poly-lactic-*co*-glycolic acid (PLGA), can tailor their use towards biomedical applications.

One application of thread-based biosensors is continuous glucose monitoring (CGM). CGM systems measure glucose levels in interstitial fluid (ISF) and convert those measurements to blood glucose concentration.[12] Compared to other flexible bioelectronic platforms that are realized on two dimensional planar polymeric substrates, threads are one dimensional and thus capable of three-dimensional tissue embedded sensing, which is ideal for small animals such as house sparrows.[1–6,11,13–25] Although CGM has been implemented in a range of laboratory and captive animals for studies on diabetes,[26–29] real-time monitoring in free-living species extends beyond medical research. However, CGM has yet to be

[a]Department of Chemical and Biological Engineering, Tufts University, Medford, MA, 02155, USA. E-mail: sameer.sonkusale@tufts.edu
[b]Nano Lab, Advanced Technology Laboratory, Tufts University, Medford, MA, 02155, USA
[c]Department of Biology, Tufts University, Medford, MA, 02155, USA
[d]Department of Electrical and Computer Engineering, Tufts University, Medford, MA, 02155, USA
[e]Department of Biomedical Engineering, Tufts University, Medford, MA, 02155, USA

†Electronic supplementary information (ESI) available. See DOI: https://doi.org/10.1039/d3an01488f

‡These authors contributed equally to this work.

explored in free-living species due to difficulties of measuring and transmitting data over the long distances travelled in flying or diving animals.[30,31] Moreover, current methods for monitoring glucose levels in free-living small animal species are invasive and require multiple interactions with the animal (*e.g.*, collecting blood samples at a few time points using a point-of-care device). Capturing and handling the animals to perform sampling restrict natural behaviour, produce stress artifacts, and may miss the fluctuation in glucose response. Therefore, a less invasive and continuous monitoring method to improve animal welfare and accuracy of glucose measurements is a needed ideal alternative. It is for this reason we propose a thread-based sensor for flexible tissue-embedded sensing in captive live birds such as house sparrows.

House sparrows are relatively small birds that weight 24–39.4 g with a total length of ~16 cm. So, any flexible bioelectronic platform to be implanted in such small species should not be bulky (less than 5% of bodyweight). In addition, these sensors are meant to be implanted transdermally to achieve high signal-to-noise ratio and continuous real-time monitoring, which adds more constraints. For example, implantation should not cause harm or injury to the bird and should not alter its natural behaviour. We believe lightweight functionalized threads would address these challenges. Compared to microneedles, which would be an alternate approach, there will be less motion artifact and no chance for it to be displaced or peeled off from the body.[32,33] Different animals have different skin thicknesses, and birds have relatively thin skin compared to mammals (humans, mice, *etc.*). Therefore, microneedles could penetrate through all the bird's skin layers, eliminating the non-invasiveness aspect of microneedles. However, it is incredibly challenging to realize flexible conductive coating on threads for realization of sensors and interconnects. Prior work relied on carbon coating using dip and dry approach, which compromised the flexibility of the treads.[2,34–37] Therefore, it is more desirable to realize metallic conductive electrodes using noble metals such as gold. Furthermore, dealing with rough and intricate curved surfaces, such as threads, presents an additional challenge because of the significant likelihood of uneven coating and the potential for the active coating to flake off. This manuscript attempts to address these challenges by realizing an innovative process for gold-coated glucose-sensing flexible threads for tissue-embedded sensing in birds.

We chose to realize glucose sensing threads/sutures in this paper. Glucose regulation is a key indicator of various biological processes, nutritional state, and energy usage in free-living flying wildlife species.[30,38–40] CGM in free-flying species would provide valuable insights into the complex energy dynamics of the high energetic demands of their internal and external state. CGM provides ample data for individual repeatability and allows for individuals to act as their own controls. Monitoring glucose levels in individuals, and therefore their energy usage, links behaviour to individual fitness. For example, monitoring glucose in well-characterized avian species (*e.g.* house sparrows) offers insights into energy mobilization and regulation during a stress response, which has implications for both ecological and physiological research.[41] Understanding how individual animals respond to natural or unpredictable stressors could indicate how animals are coping in their environments, and become a valuable tool for conservation, rehabilitation, and translocation of endangered or threatened species.

In this study, we realize lightweight, flexible sensing sutures for glucose monitoring using electrochemical principles. The conductive layer on the working and counter electrodes is gold that is achieved *via* solution-based electroless deposition and plating[42] of colloidal gold,[43] which produces a more uniform and cohesive coating layer of gold on a thread's rough, uneven surface. Compared to other conductive coatings, such as carbon which requires multiple coatings for adequate conductivity, electroless deposition of gold produces a more flexible conductive suture. In addition to the conductive layer, an electron-mediating layer (Prussian blue) is electrically deposited, and enzyme–chitosan bilayers are coated.[44] Glucose oxidase, which is the enzyme immobilized in the enzyme–chitosan matrix, catalyzes the oxidation of glucose in the presence of oxygen and, as a result, alters the current in the system,[44] which is then measured using electronic circuitry and communicated wirelessly if needed.

We demonstrate the functionality of sensors by obtaining calibration curves and test data for real-time glucose monitoring, sensor stability, sensor repeatability, and analyte interference. The sensing sutures had a sensitivity value of 36.23 nA mM^{-1} within a range from 0.62 mM to 36.4 mM glucose and a limit of detection (LOD) of 0.62 mM. The sensors were able to successfully monitor changes in glucose concentration over a period of 40 minutes and remain stable for at least five days. In addition, the sensors showed selectivity towards glucose, even in the presence of other molecules. Tests on euthanized house sparrows were performed to validate sensor function in an *ex vivo* environment and small animal species. While glucose monitoring has been reported in this manuscript, sensing sutures can be expanded to the monitoring of other analytes, such as lactate, electrolytes, chemokines, and metabolites. Future efforts will integrate these sensing sutures with miniaturized wireless electronics for real-time monitoring in birds.

Materials and methods

3-Aminopropyltriethoxysaline (APTES), potassium chloride (KCl), hydrochloric acid (HCl, ACS reagent 37%), potassium ferricyanide [$K_3Fe(CN)_6$], iron chloride hexahydrate ($FeCl_3$), chitosan (high molecular weight), glutaraldehyde solution (50 wt% in water), hydroxylamine hydrochloride, sodium citrate tribasic dihydrate, tetrachloroauric(III) acid trihydrate ($HAuCl_4{\cdot}3H_2O$), and acetic acid were all purchased from Sigma Aldrich and used as received. Isopropyl alcohol 99% (IPA) was purchased from Florida Laboratories and used as received.

Methanol was purchased from Fischer Chemical and used as received. Dulbecco's Phosphate Buffered Saline (1×, PBS) was purchased from Gibco and used as received. Glucose oxidase (GOD) was purchased from Toyobo and used as received.

Polysorb™ 5-0 braided absorbable sutures were purchased from Covidien (Medtronic, USA). The heated ultrasonic cleaner (sonicator) was purchased from Sharpertek. The potentiostat used (Electrochemical Workstation) and the commercial Ag/AgCl reference electrode used were both purchased from CH Instruments, Inc. Anton Paar Litesizer 500 Particle Analyzer was used for dynamic light scattering (DLS). Oxygen plasma treatment was done in a plasma chamber from Plasma Etch, Inc. The laboratory rotator oscillator used was a TYZD-IIIA Oscillator model. The ultraviolet-visible spectrometer used was an Evolution 220 UV-Visible Spectrometer and was purchased from Thermo Scientific. Fourier transform infrared (FTIR) spectroscopy were performed using a Nicolet 6700 FTIR with an iTX attachment (Thermo Scientific).

Synthesis of gold nanoparticles (Au NPs)

1.0 wt% sodium citrate trihydrate is added to boiling 2.5×10^{-4} M hydrogen tetrachloroaurate(III) acid trihydrate to make a 3.0 vol% solution. The solution is then heated until the color changes to a deep red color, then stirred for an additional 30 minutes. The synthesized Au NP solution is stored at 4 °C when not in use.

Coating sutures with gold (electroless deposition of gold)

Sutures (5-0) were first submerged in IPA and sonicated for 10 minutes. Then, the sutures were transferred for oxygen plasma treatment for 10 minutes. Once plasma treatment was done, the sutures were then submerged in a 0.20 M APTES in methanol solution and stirred overnight (not more than 24 hours).

The sutures are then taken out of the methanol/APTES solution and rinsed three times with methanol, then three times with DI water. This step is crucial to ensure the removal of unbound APTES from the surface of the suture. Then, the sutures are transferred to a Petri dish where 4.0 mL of Au NP solution is added (volume is dependent on the size of the Petri dish). The Petri dish is then transferred onto a rotator oscillator for 25 minutes.

Once the 25-minute shaking step is over, the sutures are transferred to a new Petri dish for the gold-plating step. In this step, 3.95 mL of DI water and 1.0 mL of 5.0 mM $H_7AuCl_4O_3$ is added to the fresh Petri dish with the sutures. This step is followed by the addition of 50 mL of 40.0 mM hydroxylamine hydrochloride to the same Petri dish. The Petri dish is then transferred onto the rotator oscillator to stir for 25 minutes. This gold plating step (adding DI water, $H_7AuCl_4O_3$, hydroxylamine hydrochloride, then oscillating for 25 minutes) is repeated two more times (a total of three times). The absorbance of gold layer as a function of time is shown in Fig. S1† (one cycle). The sutures are eventually rinsed with DI water and dried off with nitrogen gas.

Coating sutures with Prussian blue

Prussian blue (PB) is deposited onto the gold-coated sutures *via* an electro-assisted process where Prussian blue is reduced onto the surface of the sutures. In a 0.10 M KCl/0.010 M HCl solution, potassium ferricyanide and iron trichloride are added (to achieve a 2.0 mM concentration of each of the solutes in the KCl/HCl solution). This solution is used as the medium in a 3-electrode system where one gold-coated suture is the working electrode, another gold-coated suture is the counter electrode, and an Ag/AgCl is the reference electrode. For the electrodeposition of PB, a cyclic voltammetry (CV) measurement is carried out onto the gold-coated suture (working electrode) by sweeping the voltage from −0.10 V to 0.40 V at a scan rate of 50.0 mV s^{-1} in 0.010 V intervals and 7.0 sweep cycles. The suture is then rinsed with DI water and dried off with nitrogen gas.

Chitosan–glucose oxidase bi-layer coating

The PB-coated suture is then dipped in a 1.0% chitosan in acetic acid and water solution for 5 minutes, rinsed in 1× PBS, dipped in 20.0 mg mL^{-1} solution of glucose oxidase (GOD) in 1× PBS for 5 minutes, then rinsed in 1× PBS again. This creates one bi-layer of chitosan–glucose oxidase on the suture. This step is repeated 5 times (6 bilayers in total). Once the bilayers are coated, the suture is dipped in a 2.5% solution of glutaraldehyde (GA) in water for 5 minutes, rinsed in 1× PBS, then dried with nitrogen gas. The suture is stored in a 4 °C refrigerator to preserve the enzyme layers for later use.

Flexibility studies

To assess the range of flexibility in which the conductivity of the thread remains intact and does not deviate from the starting resistance, we measured the change in resistance after flexing 3 cm long gold coated thread around 2.0 cm, 1.5 cm, and 1.0 cm radii of curvature. Eutectic gallium–indium (EgaIn) contacts were added on to the ends of threads and connected to multimeter. The baseline, non-flexed 3.0 cm thread resistance was first measured. The thread was flexed at 2.0 cm radius of curvature for 10 seconds then returned to a straight position for remeasurement of resistance. These steps were repeated for 1.5 cm and 1.0 cm radii of curvature on three different threads. The resistance was compared pre- and post-flexing to determine the maximum flexibility affordable to maintain reliability of the threads' conductivity.

To assess the range of flexibility of glucose detection and effect of flexibility on the immobilized enzyme layering, the above process was repeated on a glucose sensing suture taking chronoamperometric measurements with a benchtop potentiostat with known concentration of glucose instead of taking resistance measurements. Measures of glucose concentrations were taken prior to flexing and post flexing and the change in current at baseline and at known glucose concentration was measured and compared pre-and post-flexing.

Chronoamperometric measurements

Sensor calibration, interference, stability, and repeatability tests as well as real-time glucose monitoring were all conducted using chronoamperometry. All these tests were conducted in a beaker containing 1× PBS with a stir bar and a conventional three-electrode system using a potentiostat. The three-electrode system is comprised of a GA/chitosan/GOD/PB/Au-coated suture as the working electrode (WE), and Ag/AgCl as a reference electrode (RE), and an Au-coated suture as a counter electrode (CE). In each test, volumes of known analyte concentration in 1× PBS were pipetted into the beaker to achieve the desired concentration, then chronoamperometry is run for 90 seconds with −0.20 V applied voltage. For each analyte concentration, the average current last 10 seconds of the run is calculated and reported except for the real-time glucose monitoring and the interference tests. In the real-time glucose monitoring test, the glucose concentration is increased every 10 minutes for 40 minutes. In the interference test, a different analyte is introduced every five minutes for 25 minutes.

Glucose monitoring in euthanized house sparrows

To validate sensor function in small animal species, the sensor performance was evaluated in euthanized house sparrows by infusing known glucose concentrations. Herein, a two-electrode set-up was used with the sensor (GA/chitosan/GOD/PB/Au-coated suture) as a WE and an Ag/AgCl suture as a CE/RE. These Ag/AgCl sutures were fabricated using methods previously described.[2] For implantation, we made a small incision (~2.0 mm) near the base of the neck within the dorsal featherless tract of the euthanized bird and implanted two 2.0 cm-long silastic tubes subcutaneously. Each electrode was inserted into a silastic tube to keep them separated. The incision was sutured to secure the sensing threads in place. Then, sterile saline was injected near the incision site. A baseline signal was recorded 30 minutes after saline was injected by connecting the sensor to the potentiostat. Then, known glucose concentrations were injected and measured the response as described above.

Results and discussion

Characterization of gold nanoparticles (Au NPs)

The smaller the size of Au NPs, the more the surface coverage, that will in turn result in faster and uniform electroless deposition of gold on rough thread surface, to be carried out in next step, for improved conductivity. Dynamic light scattering (DLS) measurement confirmed that the synthesized Au NPs have a hydrodynamic diameter of 43.36 ± 1.11 nm with a polydispersity index (PDI) of 24.90 ± 0.70%. This confirms that the size of Au NPs was less than 50.0 nm, resulting in a uniform surface coverage as depicted in Fig. 1c and e.

Gold coating and Prussian blue deposition

The layers coating the suture were deposited in the following order: gold, PB, and six bilayers of chitosan–glucose oxidase (illustrated in Fig. 1a). Fig. 1b–d show optical microscope

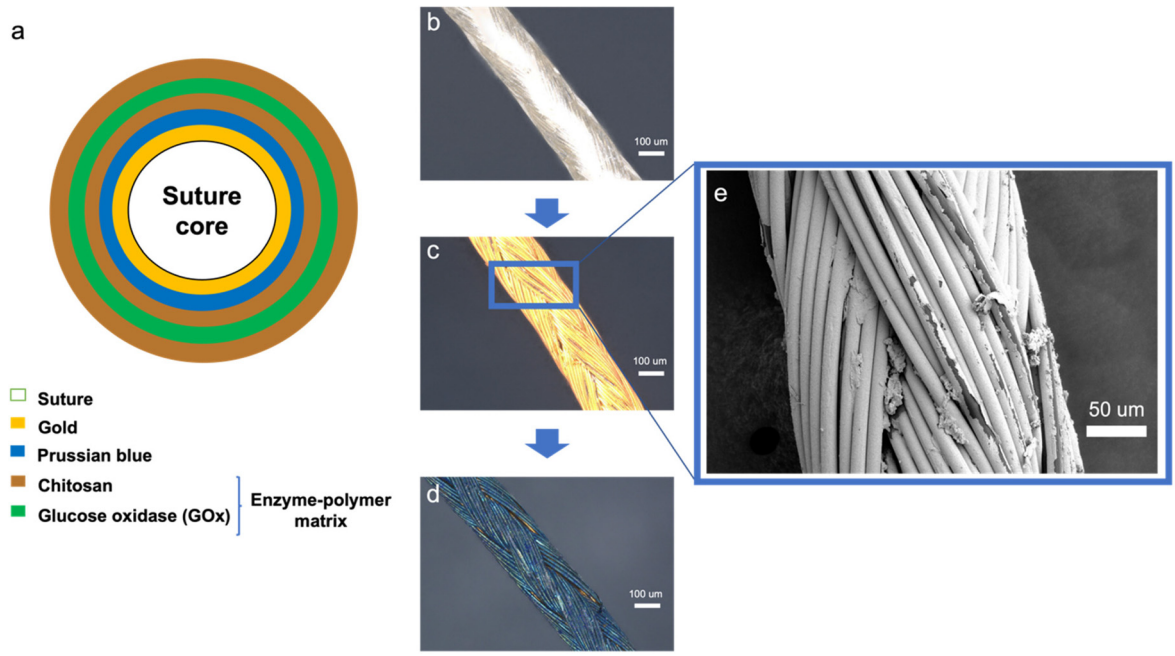

Fig. 1 Sensor layers and characterization. (a) A schematic showing a sensor's cross-section with conductive layers (gold and Prussian blue) and enzyme-immobilization layers (chitosan and glucose oxidase). Microscopic images of (b) pristine Polysorb™ suture (COVIDIEN 5-0), (c) the suture coated with gold, and (d) the suture coated with Prussian blue (blue arrows represent an order of coating sequence). (e) A scanning electron microscopy (SEM) image of the gold-coated suture.

images of the suture and the gold and PB layers. Fig. 1e shows an SEM image of the gold-coated suture. This suture was not sputter coated with gold or any other conductive metal before imaging. Instead, the electroless deposition of gold formed a layer that was conductive enough to result in an SEM image. The light parts of the suture represent the areas covered with gold, and the dark parts represent ones where gold was not deposited or peeled off before taking the image. Additionally, an EDS measurement was taken on the same spot. The resulting EDS spectrum, shown in Fig. S2,† confirms the presence of carbon (0.25 keV), oxygen (0.50 keV), and gold (0.21 keV) on the gold-coated suture. The parameters used for PB deposition can be found in the ESI.† Fig. S3† shows the corresponding cyclic voltammetry plot, which also shows the corresponding redox signal at 0.165 V and 0.145 V of PB on the gold-coated suture surface. The redox behavior is similar to what has been previously reported.[44]

Fourier transform infrared (FTIR) spectroscopy

The step-by-step surface modification of suture was verified by FTIR. The FTIR spectrum of the gold-coated suture (Au-NP) in Fig. 2a shows absorption bands at 597, 1292, 1416, and 1749 cm^{-1} which correspond to the citrate capped gold nanoparticles on the suture. Fig. 2b shows a vibrational band at 2066 cm^{-1} which corresponds to the C≡N stretching with a weak, broad band around 3292 cm^{-1} that confirm the presence of Prussian blue on the suture. In Fig. 2c, vibrational bands at 1520, 1630, 2841, and 2910 cm^{-1} correspond to the presence of amide (NH), C=C double bonds, and the stretching of CH2 which confirm the presence of glucose oxidase.[45] The additional peaks at 1390 cm^{-1} (bend., imide) further confirms the successful modification of surface. The suppression of the C≡N vibration band with a small shift to 2073 cm^{-1} confirms that surface has been completely modified with the enzyme layer.[45]

Flexibility studies

Fig. 3a–d shows the gold-coated suture being flexed to 2.0, 1.5, and 1.0 cm. Fig. 3e shows the normalized change in resistance as a function of radius of curvature (extent of bending). The length of the suture was 3.0 cm, hence the normalized change in resistance is at 0 when the radius is 3.0 cm (initial point). As the suture is bent, the resistance increases, and the normalized change in resistance increases. The increase in resistance due to bending is due to the creation of gaps within the gold layer of the surface of the suture, which decreases the conductivity.

Fig. 3f–I shows the enzyme-immobilized suture being flexed to 2.0, 1.5, and 1.0 cm. Fig. 3j shows the current measured at known glucose concentrations (0.10 and 0.30 mM). It is evident that the performance of the sensor is not disrupted by flexion down to 1.5 cm but begins to change past that flexion point. These results show that the suture is reliable in conductivity and glucose detection while flexed up to 67% flexion. When implanted in birds, the flexion is expected to be less than 10% and hence this level of performance is more than adequate.

Sensor calibration and real-time glucose monitoring

The sensor performance was evaluated in an *in vitro* environment. The sensor calibration was obtained by changing the concentration of glucose in 1× PBS from 0 to 36.4 mM and recording the current for each glucose concentration. Fig. 4a shows the calibration curve for the glucose sensor. The sensor showed a linear range from 0.62 to 36.4 mM glucose with a correlation coefficient (R^2) of 0.9978 (n = 4). Based on the obtained calibration curve, limit of detection (LOD) for the sensor is 0.62 mM glucose in 1× PBS. The sensor's sensitivity within the 0.62–36.4 mM concentration range is 36.23 nA mM^{-1}. The blank concentration (0 mM) was assumed to be 1 order of magnitude lower than the next lowest concentration to be included on the x-axis of Fig. 4a.

For continuous glucose measurements, the concentration of glucose was changed from 0 to 0.30 mM in intervals of 0.10 mM per 10 minutes while the potentiostat was continuously recording the current (shown in Fig. 4b). The current for 1× PBS before the addition of any glucose was 2.15 nA (blank). The current then increased to ~2.48 nA, ~2.81 nA, and ~2.98 nA when the glucose concentration increased to 0.10 mM, 0.20 mM, and 0.30 mM, respectively.

Interference test

To test the selectivity of the sensor to glucose in the presence of structural and non-structural co-contaminants, a sensor

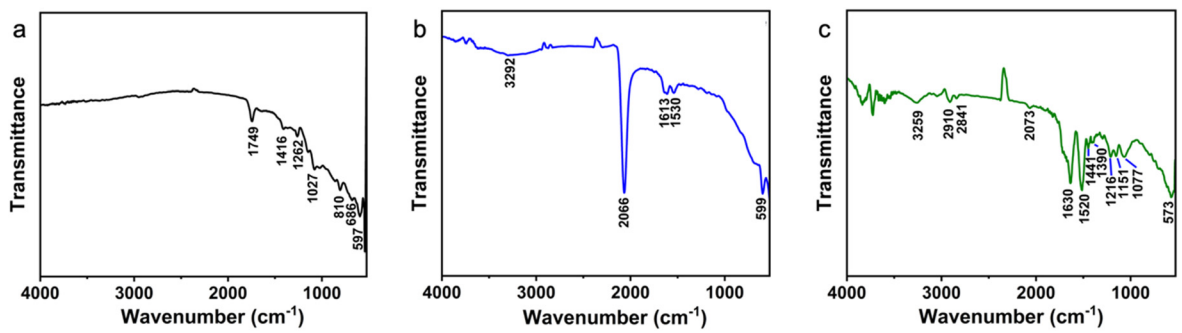

Fig. 2 FTIR spectra for (a) gold-coated suture, (b) Prussian blue-coated suture, and (c) enzyme-polymer matrix-coated suture.

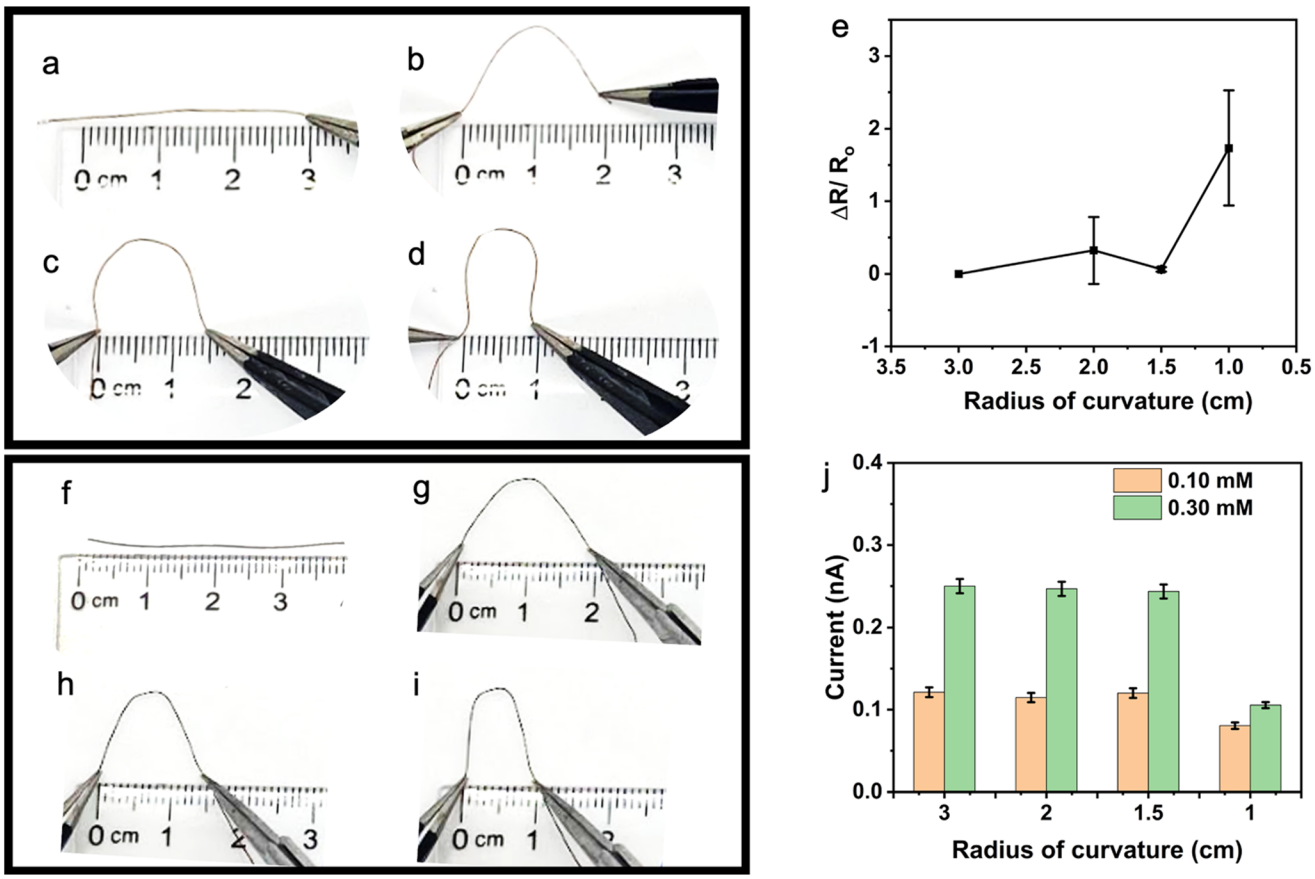

Fig. 3 (a–d) bending a gold-coated suture to radii of curvature of 2.0, 1.5, and 1.0 cm from its original 3 cm length. (e) Normalized change in resistance as a function of radius of curvature. (f–i) Bending a glucose sensing suture (fully functionalized) to radii of curvature of 2.0, 1.5, and 1.0 cm from its original 3.0 cm length. (e) Normalized change in resistance as a function of radii of curvature (n = 3, multiple sensors) (j) current readout for two different glucose concentrations (0.10 mM and 0.30 mM) as a function of radius of curvature (n = 3, multiple sensors).

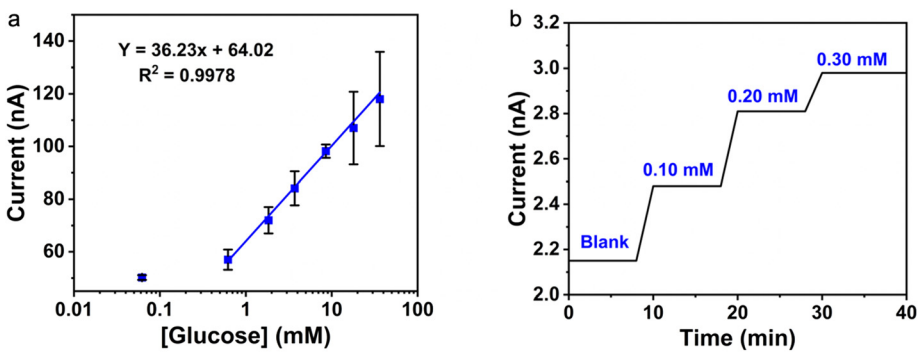

Fig. 4 Sensor calibration and real-time glucose monitoring: (a) sensor calibration curve showing the change in current with changing glucose concentration in 1× PBS-based solution (n = 4, one sensor). (b) Real-time glucose sensing by monitoring the current as the glucose concentration was increased every ~10 minutes (0, 0.10, 0.20, then 0.30 mM glucose in 1× PBS).

interference test was run to test the interference of lactate, NaCl, and KCl on the sensor (shown in Fig. 5a). The sensor gave a current readout of 3.29 nA as a baseline signal. After five minutes of incubation in 1× PBS, glucose was added to the solution to achieve 0.10 mM total glucose concentration. At 0.10 mM total concentration of glucose, the current read by the sensor increased to ~3.75 nA and stayed constant until the next analyte was added. At the 10-minute mark, lactate was added to the solution to achieve a total concentration of 18.0 mM lactate. With the addition of lactate, the sensor current readout increased to 3.83 nA. Adding NaCl (18.0 mM total NaCl concentration) at the 15-minute mark increased the

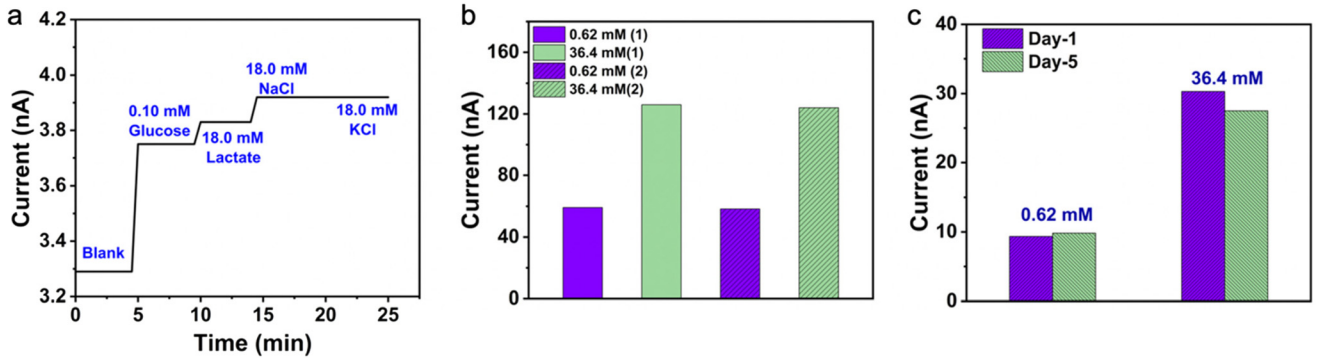

Fig. 5 Sensor interference, repeatability, and stability tests. (a) Sensor interference/selectivity test showing the change in current in 1× PBS and after the addition of 0.10 M glucose, 18.0 mM lactate, 18.0 mM NaCl, and 18 mM KCl (added sequentially with five-minute intervals). (b) Sensor repeatability test showing the current read by the sensor in 0.62 mM glucose (first measurement), 36.4 mM glucose (first measurement), 0.62 mM glucose (second measurement), then 36.4 mM glucose (second measurement). (1) and (2) in the legend of b represent the first and the second measurement, respectively, obtained for each of the two glucose concentrations. (c) Sensor stability showed as a comparison between the current read by the sensor for two glucose concentrations (0.62 and 3.71 mM glucose) on days one and five from sensor fabrication.

current to 3.92 nA. And adding KCl (18.0 mM total KCl concentration) at the 20-minute mark did not change the current readout. The selectivity studies demonstrates that even though the sensor current readout changed with the addition of lactate and NaCl, the change in current due to glucose (4.6 nA mM^{-1} glucose) is about three orders of magnitude higher than the change in current due to lactate (0.00444 nA mM^{-1} lactate) and to NaCl (0.005 nA mM^{-1} NaCl).

Sensor repeatability and stability

As depicted in Fig. 5b, the sensor precision was verified by testing at two different glucose concentrations (0.62 mM and 36.4 mM) in the following order: 0.62 mM, 36.4 mM, 0.62 mM (second test), then 36.4 mM (second test). The first and second 0.62 mM chronoamperometry tests gave current readouts of 59.2 nA and 58.3 nA, respectively. The percentage difference

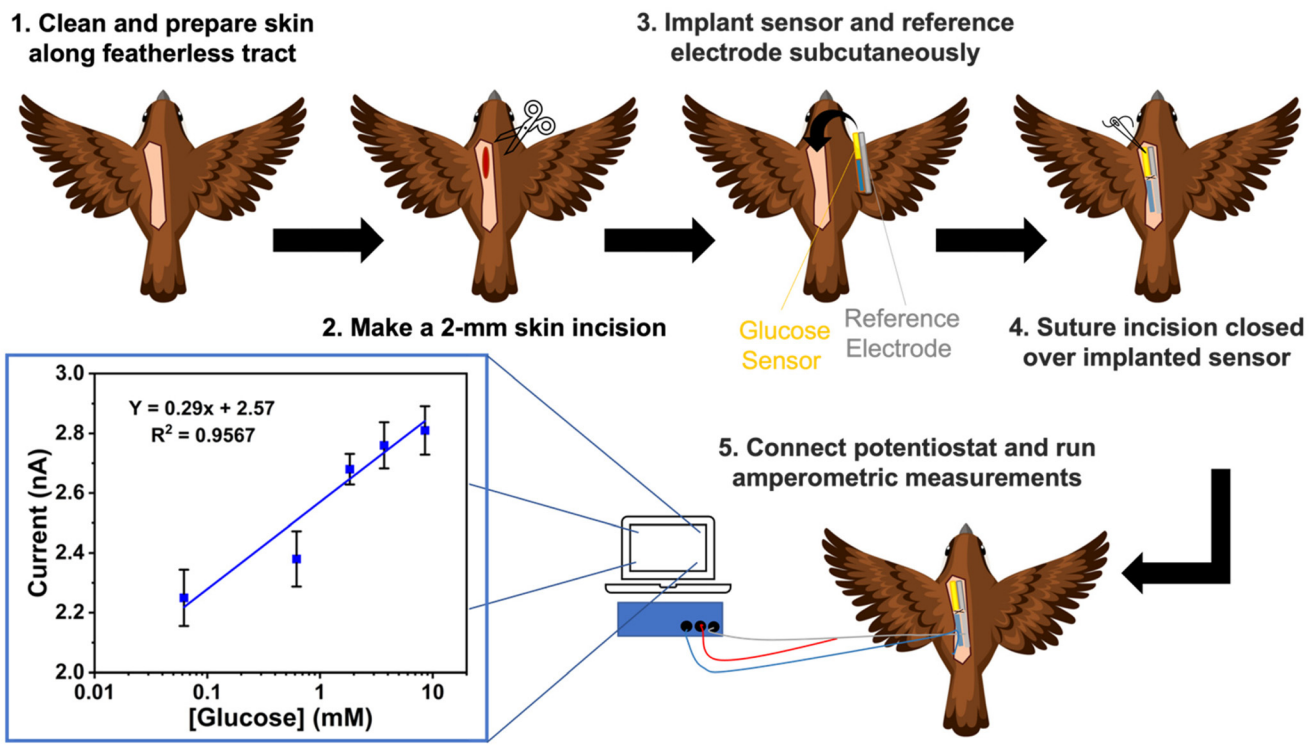

Fig. 6 Glucose monitoring in euthanized house sparrows (*Passer domesticus*) (n = 3, multiple sensors). Chronoamperometric measurements were obtained by a two-electrode system implanted in house sparrows for monitoring glucose. The concentration of glucose around the sensing region was changed by infusing 1× PBS–glucose solutions of known concentrations (x-axis) and the current was recorded after each infusion.

between both measurements is a 1.50% drop in the current. This pair of tests suggest that the change in concentration from 0.62 mM to 36.4 mM and then back to 0.62 mM does not affect the performance of the sensor. The first and second 36.4 mM tests gave current readouts of 126 nA and 124 nA, respectively. The percent difference between both measurements is a 1.60% drop in the current. This pair of tests also suggest that the change in concentration from 36.4 mM to 0.62 mM and then back to 36.4 mM does not affect the performance of the sensor. Such a test is important to ensure consistency in the sensor's performance in environments with fluctuating glucose concentrations. The sensor's stability was tested within a span of five days from fabrication (Fig. 5c). On day one, the chronoamperometry measurement of PBS–glucose solutions resulted in current readouts of 9.34 nA and 30.3 nA for 0.62 mM and 3.71 mM, respectively. Day five tests resulted in current readouts of 9.82 nA and 27.5 nA for 0.62 mM and 3.71 mM, respectively. The percent change in the current readout between the first and fifth day was a 5.1% increase and a 9.0% drop for 0.62 mM and 3.71 mM, respectively. This drop in signal over 5 days is less than 10.0%, which is under statistically significant acceptable limit.

Glucose monitoring in euthanized house sparrows

The procedure of implanting the sensor in euthanized house sparrows and the glucose sensing test results are shown in Fig. 6. Fig. 6 shows the increases in current that correspond to the spikes of glucose in the house sparrows. The changes were detected from baseline (0 mM) to the addition of 8.55 mM of glucose total, with an overall increase of current from 2.25 to 2.81 nA. In house sparrows and similar bird species, such as the European starling, this range of change is typical of the change in blood glucose levels birds experience throughout the day or in baseline to stress-induced levels.[46,47] Fig. 6 also shows an R^2 of 0.9567, and a slope of 0.29 nA mM^{-1}, which corresponds to the sensor's sensitivity in the euthanized bird. Similar to Fig. 4a, the blank concentration (0 mM) was assumed to be 1 order of magnitude lower than the next lowest concentration to be included on the *x*-axis of Fig. 6. These results reveal that these sensors function as expected and detect changes in glucose concentrations in the tissue environment of house sparrows.

These results overall prove the possibility of fabricating gold-coated sutures that could be further functionalized to produce flexible electrochemical sensors for detecting biomarkers other than glucose, such as lactate. The results also prove the viability of such sensors *ex vivo*. Moving to *in vivo* studies will need parallel effort to miniaturize the size and weight of the electronics module for readout, which will be basis of future work. After which, further studies can be done on *in vivo* animal models and possibly freely moving/flying house sparrows in natural habitat.

Conclusions

Thread-based biosensors are a promising alternative to rigid, bulky implantable sensors. Specifically, they offer a less invasive alternative for the continuous monitoring of biomarkers in small animal species, such as avian species, by simply stitching smart sutures transdermally into the skin tissue. Transdermal, stitched-in-place smart sensing sutures are expected to perform better in live birds than say microneedles which are prone to be misplaced due to motion. In this study, we demonstrate fabricating gold-coated, enzyme-immobilized, electrochemical glucose biosensors for transdermal implantation. We test their stability, repeatability, and selectivity. We also test them *ex vivo* in euthanized house sparrows (*Passer domesticus*). The sensors demonstrated glucose sensitivity of 5.0 nA mM^{-1} and were calibrated and tested within the expected blood glucose level in house sparrows (0–8.55 mM). Future studies include characterizing thread-based sensors in live animals, exploring other relevant biomarkers (*e.g.*, lactate), and developing lightweight wearable-electronic systems that have the potential to revolutionize ecological and physiological research and assist in the conservation and management of free-living species.

Author contributions

M.K.A., R.E.R., and A.S. contributed equally to conducting experiments, generating figures/plots, analyzing findings, and writing the manuscript. J.X. and R.E.O. advised on methodology. L.M.R. administered the project and reviewed and edited the manuscript. S.S. conceptualized the idea behind the reported work, administered and supervised the project, and reviewed and edited the manuscript. All authors approved the final version of the manuscript.

Conflicts of interest

The authors declare no conflicts of interest.

Acknowledgements

The authors would like to thank undergraduate students Alexi R. Judge (Tufts University) and Alex Lapointe (University of South Florida) for their help with experiments. The authors would also like to thank National Science Foundation (NSF) grant #1951104 and #1935555 to S. S. and #IOS1655269 to L. M. R.

References

1 J. Xia and S. Sonkusale, Flexible thread-based electrochemical sensors for oxygen monitoring, *Analyst*, 2021, **146**(9), 2983–2990.
2 T. Terse-Thakoor, *et al.*, Thread-based multiplexed sensor patch for real-time sweat monitoring, *npj Flexible Electron.*, 2020, **4**(1), 1–10.

3 M. Punjiya, *et al.*, PH sensing threads with CMOS readout for Smart Bandages. Proceedings - IEEE International Symposium on Circuits and Systems, 2017, pp. 10–13.
4 P. Mostafalu, *et al.*, A Textile Dressing for Temporal and Dosage Controlled Drug Delivery, *Adv. Funct. Mater.*, 2017, **27**(41), 1–10.
5 H. R. Nejad, A. Sadeqi and S. Sonkusale, Thread as a Precise Sampling and Delivery Platform for Implantable or Ingestible Applications. 2020. The 24th International Conference on Miniaturized Systems for Chemistry and Life Sciences (μTAS 2020).
6 R. E. Owyeung, *et al.*, Highly Flexible Transistor Threads for All-Thread Based Integrated Circuits and Multiplexed Diagnostics, *ACS Appl. Mater. Interfaces*, 2019, **11**(34), 31096–31104.
7 W. Tan, *et al.*, Go with the capillary flow. Simple thread-based microfluidics, *Sens. Actuators, B*, 2021, **334**, 129670–129670.
8 G. Acar, *et al.*, Wearable and Flexible Textile Electrodes for Biopotential Signal Monitoring: A review, *Electronics*, 2019, **8**(5), 479.
9 A. Hatamie, *et al.*, Review—Textile Based Chemical and Physical Sensors for Healthcare Monitoring, *J. Electrochem. Soc.*, 2020, **167**(3), 037546.
10 M. Stoppa and A. Chiolerio, Wearable electronics and smart textiles: A critical review, *Sensors*, 2014, **14**(7), 11957–11992.
11 P. Mostafalu, *et al.*, A toolkit of thread-based microfluidics, sensors, and electronics for 3D tissue embedding for medical diagnostics, *Microsyst. Nanoeng.*, 2016, **2**, 1–10.
12 I. Lee, *et al.*, Continuous glucose monitoring systems - Current status and future perspectives of the flagship technologies in biosensor research, *Biosens. Bioelectron.*, 2021, **181**, 113054.
13 T. Kumar, R. E. Owyeung and S. R. Sonkusale, Rapid clean-room-free fabrication of thread based transistors using three-dimensional stencil-based patterning, *Flexible Printed Electron.*, 2021, **6**(1), 015007.
14 R. E. Owyeung, S. Sonkusale and M. J. Panzer, Opportunities for ionic liquid/ionogel gating of emerging transistor architectures, *J. Vac. Sci. Technol., B: Nanotechnol. Microelectron.: Mater., Process., Meas., Phenom.*, 2020, **39**(1), 011001.
15 M. Punjiya, P. Mostafalu and S. Sonkusale, Smart bandages for chronic wound monitoring and on-demand drug delivery, Midwest Symposium on Circuits and Systems, 2017, pp. 495–498.
16 R. Owyeung, *et al.*, Free form three dimensional integrated circuits and wearables on a thread using organic eutectogel gated electrochemical transistors. *arXiv*, 2023, pre-print, arXiv:2303.02447.
17 S. Sonkusale and P. Mostafalu, Thread-based integrated functional devices, in U.S. Patent Application No. 15/749207, 2022.
18 N. Matsuhisa, *et al.*, Materials and structural designs of stretchable conductors, *Chem. Soc. Rev.*, 2019, **48**(11), 2946–2966.
19 J. C. Yang, *et al.*, Electronic Skin: Recent Progress and Future Prospects for Skin–Attachable Devices for Health Monitoring, Robotics, and Prosthetics, *Adv. Mater.*, 2019, **31**(48), 1904765.
20 A. Chortos, J. Liu and Z. Bao, Pursuing prosthetic electronic skin, *Nat. Mater.*, 2016, **15**(9), 937–950.
21 S. Park, M. Vosguerichian and Z. Bao, A review of fabrication and applications of carbon nanotube film-based flexible electronics, *Nanoscale*, 2013, **5**(5), 1727–1752.
22 J. A. Rogers, T. Someya and Y. Huang, Materials and Mechanics for Stretchable Electronics, *Science*, 2010, **327**(5973), 1603–1607.
23 D. H. Kim, *et al.*, Epidermal Electronics, *Science*, 2011, **333**(6044), 838–843.
24 C. Asci, *et al.*, Ingestible pH Sensing Capsule with Thread-Based Electrochemical Sensors, *IEEE Sens.*, 2022, 1–4.
25 M. Liu, *et al.*, Preliminary Results on Sensing Pillow to Monitor Head Movement using strain sensing threads, *IEEE Sens.*, 2022, 1–4.
26 U. Klueh, *et al.*, Continuous Glucose Monitoring in Normal Mice and Mice with Prediabetes and Diabetes, *Diabetes Technol. Ther.*, 2006, **8**(3), 402–412.
27 A. J. F. King, M. R. Kennard and M. Nandi, Continuous Glucose Monitoring in Conscious Unrestrained Mice, in *Animal Models of Diabetes: Methods and Protocols*, Springer US, New York, NY, 2020, pp. 225–239.
28 R. Korstanje, *et al.*, Continuous Glucose Monitoring in Female NOD Mice Reveals Daily Rhythms and a Negative Correlation With Body Temperature, *Endocrinology*, 2017, **158**(9), 2707–2712.
29 C. Wuyts, *et al.*, Continuous glucose monitoring during pregnancy in healthy mice, *Sci. Rep.*, 2021, **11**(1), 4450.
30 K. H. Elliott, Measurement of flying and diving metabolic rate in wild animals: review and recommendations, *Comp. Biochem. Physiol., Part A: Mol. Integr. Physiol.*, 2016, **202**, 63–77.
31 A. Morales, *et al.*, Point-of-care blood analyzers measure the nutritional state of eighteen free-living bird species, *Comp. Biochem. Physiol., Part A: Mol. Integr. Physiol.*, 2020, **240**, 110594.
32 Y. Wang, Y. Wu and Y. Lei, Microneedle-based glucose monitoring: a review from sampling methods to wearable biosensors, *Biomater. Sci.*, 2023, **11**(17), 5727–5757.
33 K. M. Saifullah and Z. Faraji Rad, Sampling Dermal Interstitial Fluid Using Microneedles: A Review of Recent Developments in Sampling Methods and Microneedle-Based Biosensors, *Adv. Mater. Interfaces*, 2023, **10**(10), 2201763.
34 Y. Jiang, *et al.*, Head motion classification using thread-based sensor and machine learning algorithm, *Sci. Rep.*, 2021, **11**(1), 2646.

35 F. Alaimo, *et al.*, Reel-to-reel fabrication of strain sensing threads and realization of smart insole, *Sens. Actuators, A*, 2020, **301**, 111741.
36 F. Alaimo, *et al.*, Wearable Flexible Touch Interface Using Smart Threads, *IEEE Sens.*, 2018, 1–4.
37 A. Sadeqi, *et al.*, Washable Smart Threads for Strain Sensing Fabrics, *IEEE Sens. J.*, 2018, **18**(22), 9137–9144.
38 L. P. McGuire, *et al.*, Determining feeding state and rate of mass change in insectivorous bats using plasma metabolite analysis, *Physiol. Biochem. Zool.*, 2009, **82**(6), 812–818.
39 A. R. Gerson and C. G. Guglielmo, Energetics and metabolite profiles during early flight in American robins (Turdus Migratorius), *J. Comp. Physiol., B*, 2013, **183**, 983–991.
40 C. Alonso-Alvarez and M. Ferrer, A biochemical study of fasting, subfeeding, and recovery processes in yellow-legged gulls, *Physiol. Biochem. Zool.*, 2001, **74**(5), 703–713.
41 L. M. Romero and J. C. Wingfield, *Tempests, poxes, predators, and people: stress in wild animals and how they cope*, Oxford University Press, 2015.
42 D. J. Monk and D. R. Walt, Fabrication of gold microtubes and microwires in high aspect ratio capillary arrays, *J. Am. Chem. Soc.*, 2004, **126**(37), 11416–11417.
43 K. C. Grabar, *et al.*, Preparation and Characterization of Au Colloid Monolayers, *Anal. Chem.*, 1995, **67**(4), 735–743.
44 B. Yin, *et al.*, Amperometric glucose biosensors based on layer-by-layer assembly of chitosan and glucose oxidase on the Prussian blue-modified gold electrode, *Biotechnol. Lett.*, 2008, **30**(2), 317–22.
45 N. I. Khan, *et al.*, An integrated microfluidic platform for selective and real-time detection of thrombin biomarkers using a graphene FET, *Analyst*, 2020, **145**(13), 4494–4503.
46 U. K. Beattie, *et al.*, The Effect of a Combined Fast and Chronic Stress on Body Mass, Blood Metabolites, Corticosterone, and Behavior in House Sparrows (Passer domesticus), *Yale J. Biol. Med.*, 2022, **95**(1), 19–31.
47 L. M. Romero and L. Remage-Healey, Daily and seasonal variation in response to stress in captive starlings (Sturnus vulgaris): corticosterone, *Gen. Comp. Endocrinol.*, 2000, **119**(1), 52–9.